Rare Metal Materials and Engineering
Volume 49, Issue 8, August 2020
Available online at www.rmme.ac.cn

Science Press

Cite this article as: Rare Metal Materials and Engineering, 2020, 49(8): 2623-2629.

ARTICLE

Structure and Mechanical Properties of Multi-Element (CrMoTaNbVTi)N Films by Reactive Magnetron Sputtering

Feng Xingguo, Zheng Yugang, Zhang Kaifeng, Zhou Hui, Hu Hanjun

Science and Technology on Vacuum Technology and Physics Laboratory, Lanzhou Institute of Physics, Lanzhou 730000, China

Abstract: (CrMoTaNbVTi)N multi-element films were deposited by direct current magnetron sputtering CrMoTaNbV mosaic alloy target and pure Ti target. The composition, structure, mechanical properties and wear behavior of the films deposited at R_N (N_2/(Ar+N_2))=0%, 10%, 20%, 30% and 40% were investigated. The results show that the (CrMoTaNbVTi)N films deposited at R_N=0% and 10% exhibit a simple bcc solid solution structure, whereas those deposited at R_N=20%, 30%, 40% show a simple fcc solid solution structure. With the increasing of R_N, the size of the surface particles decreases and the columnar crystals become denser. Meanwhile, the compressive stress, adhesive critical load (L_c), hardness and elastic modulus increase and reach maximum values of −3.3 GPa, 352 mN, 25.6±1.2 GPa and 278.8±11.2 GPa at R_N=40%, respectively. The film deposited at R_N=40% whose wear rate is decreased by about ten times compared with that of the alloy film (R_N=0%), exhibits an excellent wear resistance.

Key words: multi-element nitride film; structure; mechanical property; wear

Fifteen years ago, novel multi-element alloys were proposed by Yet et al[1,2]. Multi-element alloys films contain 5~13 major elements with concentration between 5 at%~35 at%, which can result in high-entropy, lattice distortion, sluggish diffusion and so on[3-5]. These films combine the excellent mechanical properties and superior wear resistance[6-8]. These properties make multi-element films a good solution for the applications requiring high hardness and wear resistance.

Up to now, various high-entropy alloys (HEAs) nitride films that are based on refractory metal elements (Cr, Mo, Ta, Nb, Zr, W, Ti, V, Hf, etc) have been produced. It is found that Al element frequently occurs in the majority of HEAs films, such as AlCrTaTiZr, AlCrMoTaTiZr, AlCrNbSiTiV, and TiTaCrZrAlRu[9-13]. The increase of the Al content favors the fcc to bcc phase transition and can contribute to bond between the Al and transition metals with an incompletely filled d-shell. The rest is a small amount of HEAs films that have no Al element. Pogrebnjak et al[14] synthesized (TiHfZrVNb)N coatings by the cathodic arc vapor deposition method, and demonstrated that all coatings exhibited a single cubic (NaCl-type) nitride phase and the hardness increased with the increase of bias voltage applied to the substrate. Liang et al[15] reported that all (TiVCrZrHf)N films were simple face centered cubic (fcc) structures and extreme hardness of around 48 GPa was obtained. Jayaraj et al[16] investigated TaNbHfZrTi films that exhibited high corrosion resistance. Yan et al[17] sudied the structure, electrical resistivity and thermal stability of BNbTaTiZr thin film. It was observed that the films showed amorphous structure and displayed high electrical resistivity. However, the studies about high-entropy alloys (HEAs) nitride films are mainly focused on the microstructure. The properties about wear resistance, especially for the HEAs nitride films without Al element have less been studied[18].

In the present work, transition metals Cr, V, Ta, Nb, Mo and Ti have been selected to elements of HEAs films. A novel high-entropy (CrMoTaNbVTi)N nitride films were prepared by reactive co-sputtering of CrMoTaNbV mosaic target and pure Ti target in Ar+N_2 mixed atmosphere. The films were characterized in terms of elemental and chemical composition, crystalline structure, surface morphology, residual stress,

Received date: August 25, 2019
Foundation item: National Natural Science Foundation of China (51601083)
Corresponding author: Zhou Hui, Ph. D., Professor, Science and Technology on Vacuum Technology and Physics Laboratory, Lanzhou Institute of Physics, Lanzhou 730000, P. R. China, Tel: 0086-931-4585614, E-mail: zhouhuilz510@163.com

hardness, adhesive force and wear properties.

1 Experiment

The (CrMoTaNbVTi)N nitride films were deposited by reactive co-sputtering of CrMoTaNbV mosaic target and pure Ti target. The alloy mosaic target was composed of V (99.99%), Mo (99.99%), Ta (99.99%), Nb (99.99%) and Cr (99.99%). The size of Cr and V target was 78 mm×85 mm×8 mm, and the size of Mo, Nb and Ta targets was 62 mm×85 mm×8 mm. The distance between the mosaic target and substrate was kept constant at 300 mm and pure Ti target to substrate was 450 mm. The substrates were cleaned ultrasonically in acetone and ethanol. Prior to deposition, the chamber was pumped down to a base pressure below 3×10^{-3} Pa, and then the samples were subjected to Ar^+ ions by an ion source with 1400 V for 20 min. The deposition bias voltage, working pressure and deposition time were −100 V, 0.5~0.6 Pa and 120 min, respectively. The sputtering discharge current of the mosaic target and pure Ti target was set at 2.0 and 1.5 A, respectively. The nitrogen flow ratio $N_2/(Ar+N_2)$, denoted as R_N, was varied from 10% to 40% to prepare films of various nitrogen contents.

The chemical composition of the films was obtained using EDS (FEI Quanta-200FEG) with an atomic number (Z), absorption (A) and fluorescence (F) corrected program[19]. In order to reduce uncertainties, three electron energies (30, 25 and 20 keV) were used to measure different spots. The basic error can be estimated to be 4%~6%. The crystal structures were characterized using an X-ray diffraction (XRD, D/MAX 2200) with Cu Kα radiation and a glancing incident angle of 1°. The plane-view and cross-sectional grain morphology of films were observed by field emission scanning electron microscopy (FESEM, Quanta 200FEG). The hardness and elastic modulus of these nitride films were measured by a nanoindenter with continuous stiffness measurement (CSM) technique. The penetration depth of the indenter was controlled between 1/8~1/10 of the film thickness to avoid substrate effect. The optical substrate-curvature method was used to measure the residual stress of the films. The residual stress was calculated applying the Stoney Eq. (1), where the E_s and υ_s are the Young's modulus and Poisson's ratio of the 9Cr18 steel substrate, respectively; s is the thickness of the substrate; f is the thickness of the film; $1/R$ is the curvature of the films. The friction coefficient and wear rate were measured using a ball on disc tester. All the tests were performed using a normal load (P) of 2 N, a constant sliding speed of 25.13 cm/s at 25 °C and a relative humidity of 31%. The diameter of the circle wear track (D) and the sliding distance (d) were 12 mm and 225 m, respectively. A surface profiler tested the profile of the wear track (A), and then calculated the wear rate (W) using the following Eq. (2). The 3D images were examined by a surface profilometer (Talysurf CCI) scanning across the wear track. The morphologies of the wear tracks were observed by optical microscope.

$$\sigma = \frac{1}{6R}\cdot\frac{s^2}{f}\left[\frac{E_s}{(1-\upsilon_s)}\right] \quad (1)$$

$$W = \frac{\pi DA}{Pd} \quad (2)$$

2 Results and Discussion

2.1 Chemical composition and deposition rate

Fig.1 shows the chemical composition of CrMoTaNbVTi nitride films analyzed by EDS. For the alloy films (R_N=0), the atomic fraction (at%) of Cr, Mo, Nb, Ta ,V and Ti is 14.3, 15.2, 16.7, 19.2, 14.9 and 19.7, respectively, each of which has an atomic fraction between 5 at% and 35 at%. With the introduction of nitrogen, the content of metal is obviously decreased and the nitrogen content sharply increases with increasing R_N. The N contents in the films deposited at R_N=10%, 20%, 30% are about 20.3 at%, 31.9 at% and 41.6 at%, respectively, which can be regarded as under-saturated nitride films with partially remained metallic alloys. When R_N=40%, the nitrogen content reaches up to saturated value of 48.8 at%.

Fig.2 shows the target voltage and deposition rates of CrMoTaNbVTi nitride films as a function of R_N. It is observed that the target voltage increases with the increasing of R_N. This phenomenon can be attributed to formation of metal nitrides on the target surface, which is usually defined as "target poisoning". With the increasing of R_N, the target poisoning becomes more serious which increases the equivalent resistance of cathode and anode. According to the relationship between voltage, electric current and resistance ($U=IR$), the voltage will increase as the resistance increases and electric current keeps constant. It is also found that the deposition rate initially increases from R_N=0% to R_N=20%, and then gradually decreases from 9.4 nm/min at R_N=20% to 7.3 nm/min at R_N=40%. The initial increase of deposition rate is due to addition of nitrogen atoms to the film. The reduction of the deposition rate can be attributed to the two facts. On the one hand, the sputtering yield of target decreases with the increasing of R_N. On the other hand, the sputtering efficiency

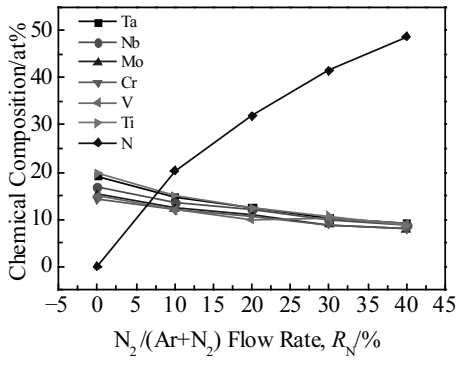

Fig.1 Chemical composition of CrMoTaNbVTi nitride films as a function of R_N

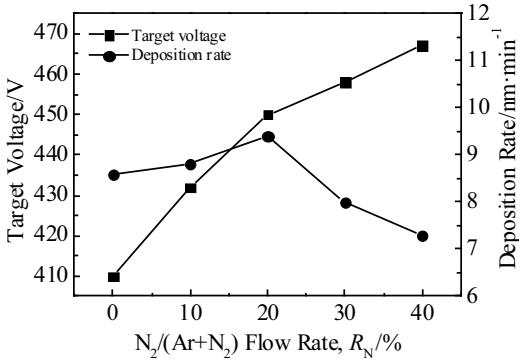

Fig.2 Deposition rate and target voltage of CrMoTaNbVTi nitride films as a function of R_N

of nitrogen ions is lower than that of argon gas ions.

2.2 XRD analysis

Fig.3 presents the XRD patterns of the films deposited at various R_N. The alloy film (R_N=0%) and the film deposited at low nitrogen flow ratio (R_N=10%) exhibit a simple bcc solid solution structure. This can be attributed to the high mixing entropy that promotes the mutual solubility of different elements in the films and prevents phase separation[20,21]. Meanwhile, Cr, Nb, Mo, Ta and V have the same bcc structures that probably enhance the bcc crystal structure formation. For the nitride films deposited at R_N=10%, the intensity of (110) peak is significantly reduced and the breadth of (110) peak increases. When R_N increases from 20% to 40%, a simple fcc structure is observed in these films. There has been no complete phase formation rule to support the study of high-entropy alloy films. The evolution from a bcc structure to an fcc structure with increasing R_N may be due to high mutual solubility and the similar structures of the nitrides. In the present system, TiN, TaN, NbN, MoN, CrN and VN are all fcc structures. It is thought that the fcc structures promote the fcc crystal structure formation for the (CrMoTaNbVTi)N films. A shift of XRD peaks to lower angles is observed with increasing N content in the films. This is considered to partly result from distortion of the lattice with increasing N content. Such an increase in lattice spacing can cause the XRD peaks shift to lower angles. In addition, the internal stress increases linearly from 0.7 GPa to 3.3 GPa with increasing N content, which may lead to the lattice spacing enlargement. It can be seen that when R_N increases from 10% to 20%, the diffraction peaks change greatly compared with from 30% to 40%. This is because the phase structure has changed when R_N increases from 10% to 20%; the (111) peak position of fcc is much lower than the (110) peak position of bcc.

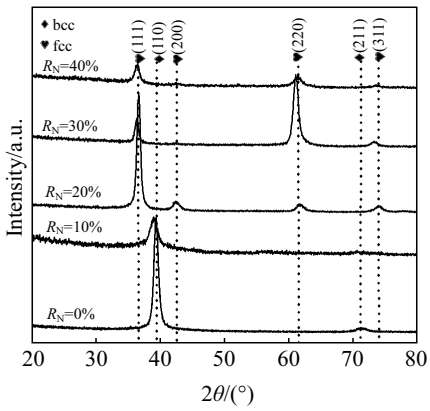

Fig.3 XRD patterns of the CrMoTaNbVTi nitride films deposited at various R_N

2.3 Surface and cross-sectional morphology

Fig.4 shows the SEM micrographs of (CrMoTaNbVTi)N films deposited at various R_N. The surface morphologies of all the films exhibit a grain-like structure and the cross-section is the typical columnar microstructure. For the metallic film (R_N=0%), the grain-like structure is composed of clusters with 60~100 nm, and many voids exist on the surface. The cross-sectional view of metallic film displays coarse columnar crystals, and the width of these columnar is around 80~100 nm. Compared with R_N=0%, the surface voids of the films deposited at R_N=10% decrease and the width of columnar becomes small. When R_N=20% and 30%, the size of the surface particles reduces to 50~70 nm and a dense columnar crystal is observed. With further increasing R_N to 40%, the average grain size is about 30 nm which is smaller than those of the other films. This is consistent with its XRD pattern that has larger full width at half maximum (FWHM). The cross-section of the films shows fibrous columns, and no distinct column boundaries and defects are observed. With the increase of R_N, the films become denser due to the enhancement of the adatom mobility.

2.4 Mechanical properties

The residual stress of (CrMoTaNbVTi)N films was measured using the substrate bending method according to Eq. (1). From Table 1, it can be seen that all the films exhibit a compressive stress, and the compressive stress increases with increasing R_N. This can be attributed to the structure stress and thermal stress. The structure stress is originated from lattice mismatch, which increases with the increasing N content. The thermal stress leads to different thermal expansion coefficients between the film and substrate.

The adhesive critical load (L_c) is defined as the load at the first surface crack in the present paper. Fig.5 shows the L_c of the film deposited at R_N=40%. It can be found that the crack appears at 352 mN. The L_c values of the films are also summarized in Table 1, which increase with increasing R_N. The adhesive critical loads are mainly influenced by hardness, residual stresses, films structure and so on. The compressive stress can enhance resistance of crack formation and the higher hardness is more resistant to plastic deformation[22,23].

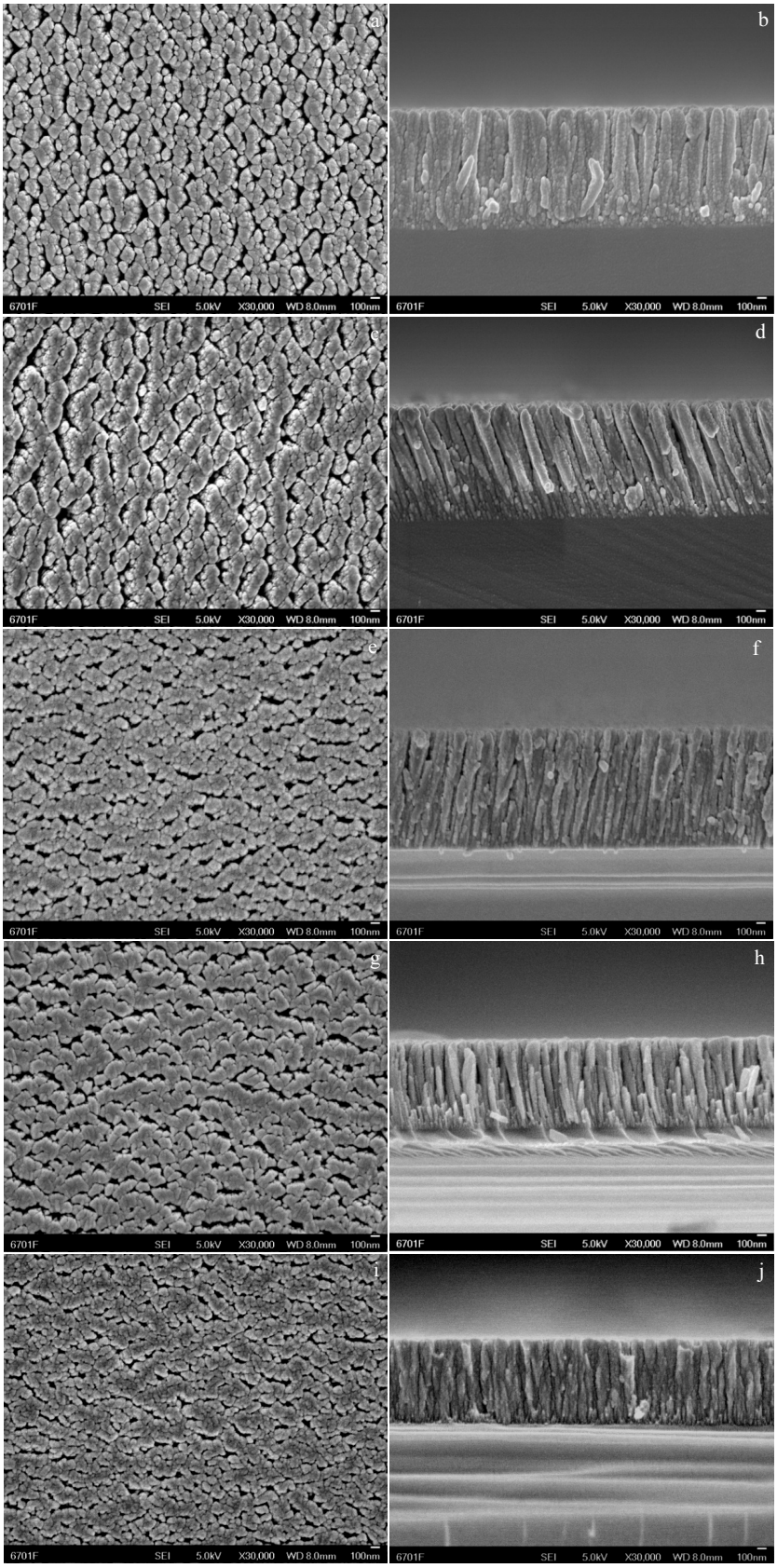

Fig.4 Plane-view (a, c, e, g, i) and cross-section (b, d, f, h, j) FESEM micrographs of CrMoTaNbVTi nitride films deposited at various R_N: (a, b) 0%, (c, d) 10%, (e, f) 20%, (g, h) 30%, and (i, j) 40%

Table 1 Compressive stress (σ), adhesive critical load (L_c), hardness (H) and elastic modulus (E) of the nitride films deposited at various R_N

R_N/%	σ/GPa	L_c/mN	H/GPa	E/GPa
0	−0.7	198	8.9±0.5	187.5±6.5
10	−1.2	291	15.6±0.7	197.5±8.3
20	−2.0	305	18.7±0.9	225.4±9.5
30	−2.4	338	22.3±1.0	251.6±8.7
40	−3.3	352	25.6±1.2	278.8±11.2

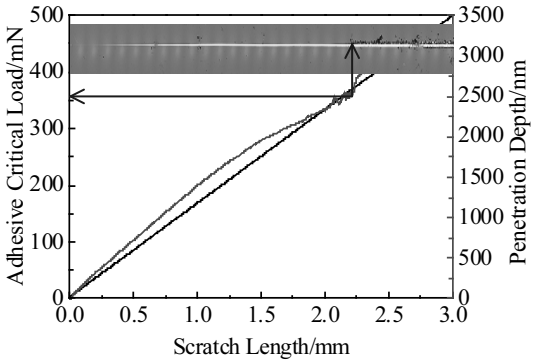

Fig.5 Scratch test results of film deposited at R_N=40%

The film deposited at R_N=40% has higher compressive stress and hardness that are more resistant to crack formation and plastic deformation, thus leading to the higher L_c. In addition, with the increase of R_N, the films become denser and the interface surface of film and substrate is better, which can enhance the adhesive critical load.

The hardness and elastic modulus of (CrMoTaNbVTi)N deposited at various R_N are shown in Table 1. For the metallic film (R_N=0%), the hardness and modulus values are 8.9±0.5 GPa and 187.5±6.5 GPa, respectively. As R_N further increases, the hardness and elastic modulus continues to increase, reaching a maximum value of 25.6±1.2 GPa and 278.8±11.2 GPa at R_N=40%, respectively. This can be attributed to three facts[24,25]. The first is the grain refinement effect. From SEM morphology, it can be found the grain size decreases with increasing R_N. The second reason is increasing Me-N nitrides in the films with increasing R_N, which can significantly enhance hardness and modulus. The third is compressive stress: the strengthening effect is increased with the increasing of compressive stress.

Fig.6 shows the friction coefficient curves for the nitride films deposited at R_N=0% and R_N=40%. It can be seen that the friction coefficient reaches a steady state after a running-in period with a sliding distance of 25 m. The average friction coefficient value of the films deposited at R_N=0% and R_N=40% is about 0.75 and 0.45, respectively. The nitride films have lower friction coefficient than the metallic film (R_N=0%), which can be due to the nitride films having lower surface roughness than the alloy film.

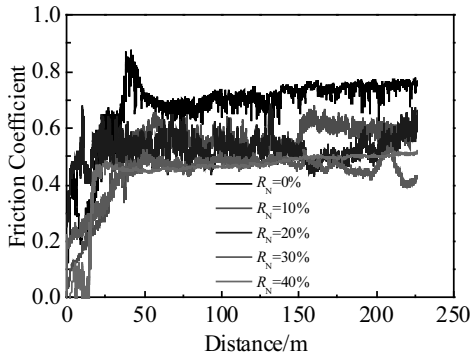

Fig.6 Friction coefficient of CrMoTaNbVTi nitride films deposited at various R_N

Fig.7 shows the cross-sectional profiles and 3D images of wear track deposited at various R_N. From the cross-sectional profiles and 3D images, it can be clearly seen that the wear track of the film deposited at R_N=40% is much narrower and shallower than that of the metallic film (R_N=0%), indicating excellent wear resistance. The wear rates of the films are listed in Table 2. It is found that the wear rate decreases with increasing R_N. For the metallic film, the wear rate is about 4.98×10^{-14} $m^3/(N\cdot m)$. As R_N increases to 40%, the wear rate reaches a minimum value of 5.25×10^{-15} $m^3/(N\cdot m)$, which is decreased by about ten times compared with that of the metallic film. This can be attributed to the two facts: firstly, with the increasing of R_N, the friction coefficient decreases and surface roughness becomes lower, thus resulting in a lower wear rate. Secondly, the film with higher R_N has a higher hardness and denser microstructure, which can enhance the cohesive strength. According to Leyland and Matthews[26], the ratio of H/E describes the long elastic strain to failure. The tribological behaviors of the coatings can be evaluated by the value of H/E. The higher the value of H/E, the better the wear resistance will be. From Table 2, it is observed that the film deposited at R_N=40% possesses the highest H/E ratio. This result is consistent with the results of wear rate. Fig.8 presents the optical microscope (OM) images of wear track and the wear scar formed on the 9Cr18 steel balls after wear test. The wear width of the film deposited at R_N=40% is much smaller than that of the alloy film. The size of wear scar on the 9Cr18 steel balls sliding against the alloy film and the film deposited at R_N=40% is 520 and 410 μm, respectively. The wear scar for 9Cr18 steel ball sliding against the alloy film is much larger than that for the 9Cr18 steel ball sliding against film deposited at R_N=40%. From Fig.8a and 8b, it can be seen that the wear mechanism of the alloy film is predominantly adhesive wear and that of the film deposited at R_N=40% is ploughing groove.

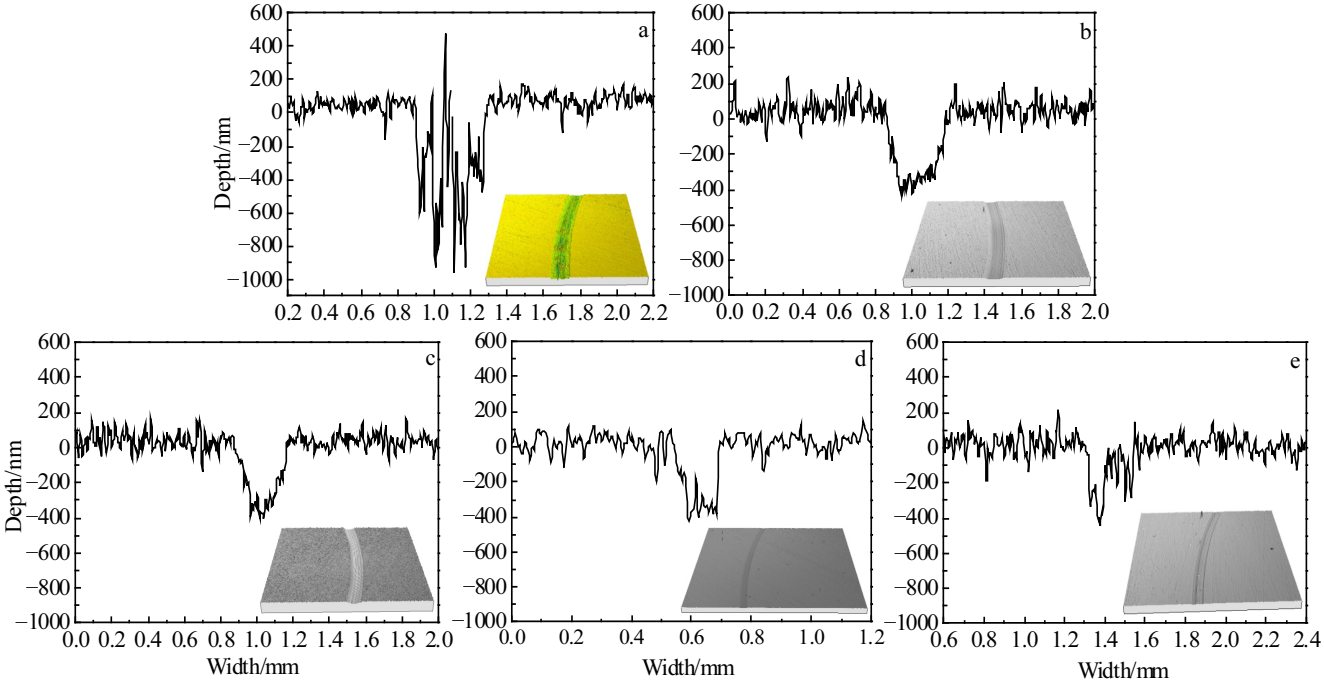

Fig.7 Cross-sectional profiles and 3D images of wear tracks: (a) R_N=0%, (b) R_N=10%, (c) R_N=20%, (d) R_N=30%, and (e) R_N=40%

Table 2 Surface roughness (R_a), friction coefficient (COF), wear rate (W) and H/E of the nitride films deposited at various R_N

R_N/%	R_a/nm	COF	W/×10^{-15} m^3·(N·m)$^{-1}$	H/E
0	8.5	0.71	49.8	0.047
10	7.6	0.55	24.7	0.078
20	7.4	0.52	9.31	0.082
30	6.8	0.47	7.68	0.087
40	6.1	0.47	5.25	0.092

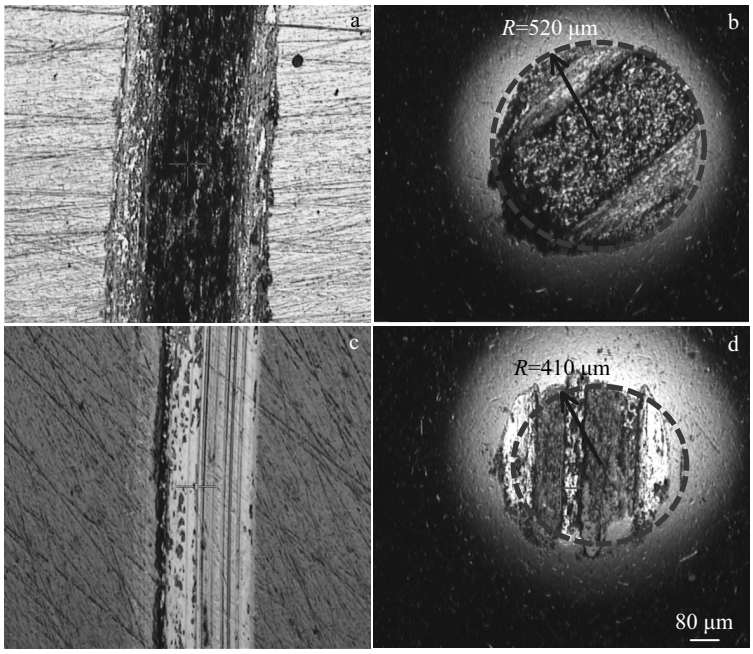

Fig.8 OM images of wear track (a, c) and wear scar (b, d) at R_N=0% (a, b) and R_N=40% (c, d)

3 Conclusions

1) The (CrMoTaNbVTi)N films deposited at R_N=0% and 10% exhibit a simple bcc structure. As R_N further increases, the structure evolves from bcc structure to fcc structure.

2) The surface morphologies of all the films exhibit a grain-like structure and the cross-section is the typical columnar microstructures. With the increasing of R_N, the grain size decreases and columnar crystals become denser.

3) With increasing R_N, the compressive stress, adhesive critical load, hardness and elastic modulus gradually increase, and reach maximum values of −3.3 GPa, 352 mN, 25.6±1.2 GPa and 278.8±11.2 GPa at R_N=40%, respectively.

4) The nitride films have a lower friction coefficient than the alloy film, and the film deposited at R_N=40% has a minimum wear rate of 5.25×10^{-15} $m^3/(N\cdot m)$, which is decreased by about ten times compared with that of the alloy film.

References

1 Yeh J W, Chen S K, Lin S J *et al. Advanced Engineering Materials*[J], 2004, 6: 299

2 Yeh J W, Chen S K, Gan J Y *et al. Metallurgical and Materials Transactions A*[J], 2004, 35: 2533

3 Niu X L, Julius J, Zhou D *et al. Rare Metal Materials and Engineering*[J], 2017, 46(12): 3621 (in Chinese)

4 Wang Y X, Yang Y J, Yang H J *et al. Materials Chemistry Physics*[J], 2018, 210: 233

5 Liu Chunhai, Pu Guo, Zhang Wei *et al. Rare Metal Materials and Engineering*[J], 2018, 47(5): 1578 (in Chinese)

6 Feng X B, Zhang J Y, Xia Z R *et al. Materials Letters*[J], 2018, 210: 84

7 Zhang Chong, Wu Bingqian, Wang Qianting *et al. Rare Metal Materials and Engineering*[J], 2017, 46(9): 2639 (in Chinese)

8 Fazakas E, Zadorozhnyy V, Louzguine-Luzgin D V. *Applied Surface Science*[J], 2015, 358: 549

9 Lai C H, Cheng K H, Lin S J *et al. Surface and Coatings Technology*[J], 2008, 202: 3732

10 Cheng K H, Lai C H, Lin S J *et al. Thin Solid Films*[J], 2011, 519: 3185

11 Huang P K, Yeh J W. *Surface and Coatings Technology*[J], 2009, 203: 1891

12 Chang S Y, Huang Y C, Li C E *et al. The Journal of the Minerals Metals & Materials Society*[J], 2013, 65: 1790

13 Tsai M H, Lai C H, Yeh J W *et al. Journal of Physics D: Applied Physics*[J], 2008, 41: 235 402

14 Pogrebnjak A D, Yakushchenko I V, Bagdasaryan A A *et al. Materials Chemistry Physics*[J], 2014, 147: 1079

15 Liang S C, Chang Z C, Tsai D C *et al. Applied Surface Science*[J], 2011, 257: 7709

16 Jayaraj J, Thinaharan C, Ningshen S *et al. Intermetallics*[J], 2017, 89: 123

17 Yan X H, Li J S, Zhang W R *et al. Materials Chemistry Physics*[J], 2018, 210: 12

18 Li W, Liu P, Liaw P K. *Materials Research Letters*[J], 2018, 6: 199

19 Goldstein J I, Newbury D E, Joy D C *et al. Advanced Scanning Electron Microscopy and X-Ray Microanalysis*[M]. New York: Plenum Press, 2003: 404

20 Chang Z C, Liang S C, Han S *et al. Nuclear Instruments and Methods in Physics Research Section B*[J], 2010, 268: 2504

21 Ren B, Shen Z G, Liu Z X *et al. Journal of Alloy and Compound*[J], 2013, 560: 171

22 Lai C H, Cheng K H, Lin S J *et al. Surface and Coatings Technology*[J], 2008, 202: 3732

23 Kuptsov K A, Kiryukhantsev P V, Sheveyko A N *et al. Surface and Coatings Technology*[J], 2013, 216: 273

24 Pogrebnjaka A D, Yakushchenko I V, Bagdasaryan A *et al. Materials Chemistry Physics*[J], 2014, 147: 1079

25 Yan X H, Li J S, Zhang W R *et al. Materials Chemistry Physics*[J], 2018, 210: 12

26 Leyland A, Matthews A. *Wear*[J], 2000, 246: 1

反应磁控溅射(CrMoTaNbVTi)N 多主元薄膜的微观组织与机械性能

冯兴国，郑玉刚, 张凯锋，周　晖，胡汉军

(兰州空间技术物理研究所 真空技术与物理国防科技重点实验室，甘肃 兰州 730000)

摘　要：采用直流反应磁控溅射方法，通过溅射镶嵌靶（CrMoTaNbV）和纯 Ti 靶制备了(CrMoTaNbVTi)N 多主元氮化物薄膜。研究了不同氮气流量比 R_N (N_2/(Ar+N_2)) 对(CrMoTaNbVTi)N 薄膜的微观结构、力学性能和摩擦学性能的影响。结果表明，当 R_N=0%和 R_N=10%时薄膜为简单的体心立方结构，当 R_N=20%，30%，40%时为简单的面心立方结构。随着 R_N 的增大，表面颗粒逐渐减小，断面柱状晶更为致密，同时(CrMoTaNbVTi)N 薄膜的残余应力、膜基结合力、硬度和弹性模量逐渐增大，且当 R_N=40%时达到最大值，分别为−3.3 GPa, 352 mN, 25.6±1.2 GPa 和 278.8±11.2 GPa。R_N=40%制备的氮化物薄膜具有最小的比磨损率，相较合金薄膜降低了约 1 个数量级，表现出优异的耐磨损性能。

关键词：多主元氮化物薄膜；微观结构；机械性能；摩擦学

作者简介：冯兴国，男，1983 年生，博士，兰州空间技术物理研究所真空技术与物理国防科技重点实验室，甘肃 兰州 730000，电话：0931-4585614，E-mail: fengxingguo10@163.com